

Supplementary Materials

Rapid and Efficient Isolation and Detection of Extracellular Vesicles from Plasma for Lung Cancer Diagnosis

Junge Chen^a, Youchun Xu^{a,b}, Xun Wang^c, Dongchen Liu^a, Fan Yang^c, Xiurui Zhu^a, Ying
Lu^{a,b,d}, Wanli Xing^{a,d,*}

^a School of Medicine, Tsinghua University, Beijing 100084, China.

^b Collaborative Innovation Center for Diagnosis and Treatment of Infectious Diseases, Hangzhou 310003, China.

^c Thoracic surgery, Peking University People's Hospital, Beijing 100044, China.

^d National Engineering Research Center for Beijing Biochip Technology, Beijing 102206, China.

* Correspondence should be addressed to W.X. (wxing@tsinghua.edu.cn)

Content

Supplementary Figures and Tables	2
Figure S1. Fluorescence image of EV-depleted plasma after DEP capture	2
Figure S2. The optimization of the DEP method.....	2
Figure S3. Size ranges and concentration of DNA extracted from isolated EVs.	3
Figure S4. Isolation of HeLa EVs from 200 μ L of simulated plasma samples by the DEP chip.	4
Figure S5. Western blotting of EVs from healthy people and lung cancer patients.	4
Figure S6. In vitro delivery of siRNA into cells by EVs isolated by DEP.	5
Table S1. The sequences of PCR primers for U6, miR-21, miR-192, miR-191 and miR-940	6
Table S2. The clinical stage and histological diagnosis of lung cancer patients.	6

Supplementary Figures and Tables

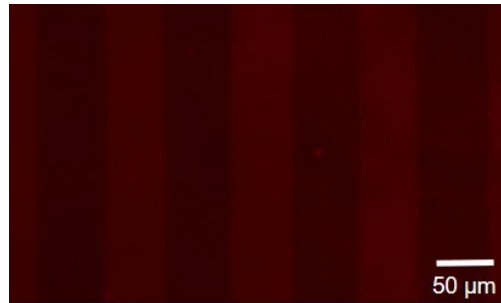


Figure S1. Fluorescence image of EV-depleted plasma after DEP capture.

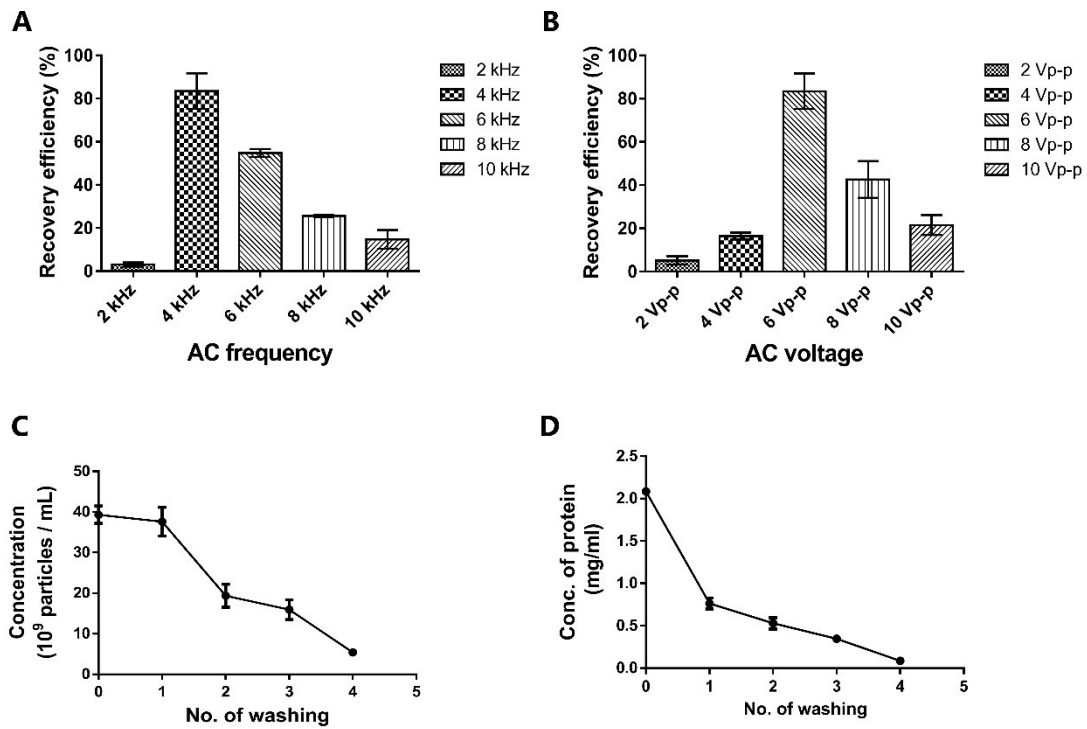


Figure S2. The optimization of the DEP method. The influence of the frequency (A) and voltage (B) of the DEP signal on the recovery efficiency was examined by NTA. (C) The influence of the number of washing on the particle concentration of EVs. (D) The influence of the number of washing on the concentration of proteins.

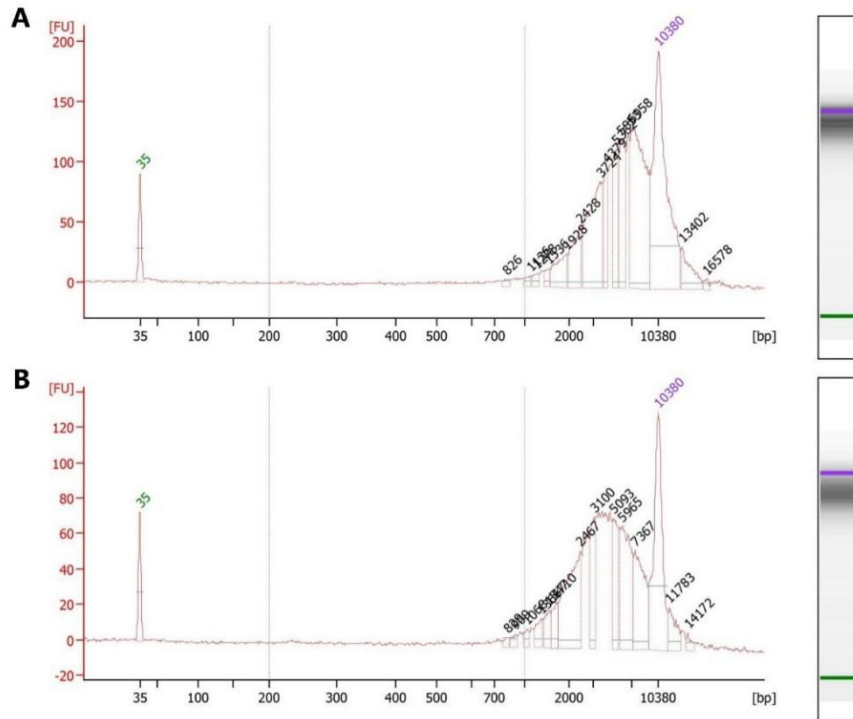


Figure S3. Size ranges and concentration of DNA extracted from isolated EVs. (A) Length distribution of DNA in EVs isolated by DEP. **(B)** Length distribution of DNA in EVs isolated by UC.

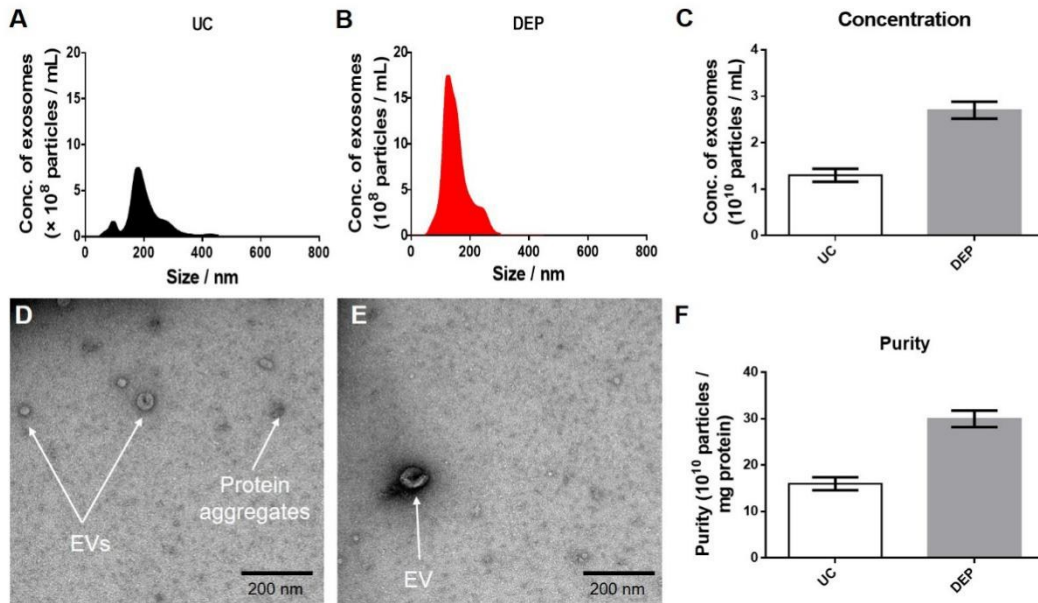


Figure S4. Isolation of HeLa EVs from 200 μ L of simulated plasma samples by the DEP chip. (A) NTA analysis of HeLa EVs isolated by UC. (B) NTA analysis of HeLa EVs isolated by DEP. (C) Concentration of HeLa EVs isolated by UC and DEP. (D) TEM image of HeLa EVs isolated by UC. (E) TEM image of HeLa EVs isolated by DEP. (F) Purity of HeLa EVs isolated by UC and DEP.

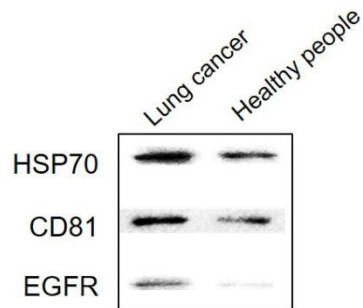


Figure S5. Western blotting of EVs from healthy people and lung cancer patients.

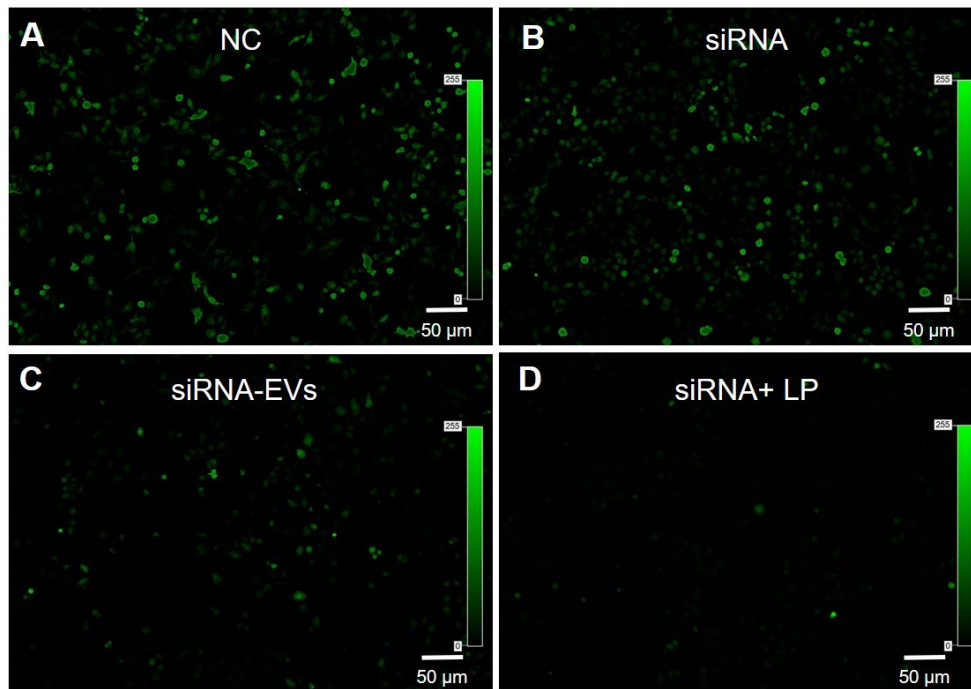


Figure S6. In vitro delivery of siRNA into cells by EVs isolated by DEP. (A) Fluorescent image of GFP-expressing HeLa cells treated with DMSO (NC). (B) Fluorescent image of GFP-expressing HeLa cells treated with siRNA. (C) Fluorescent image of GFP-expressing HeLa cells treated with siRNA-EVs. (D) Fluorescent image of GFP-expressing HeLa cells treated with siRNA+ LP.

Table S1. The sequences of qRT-PCR primers for U6, miR-21, miR-192, miR-191 and miR-940.

Target	Primer sequence
U6	CTCGCTTCGGCAGCACA
miR-21	ACACTCCAGCTGGGTAGCTTATCAGACTGA
miR-192	ACACTCCAGCTGGGCTGACCTATGAATTG
miR-191	ACACTCCAGCTGGGCAACGGAATCCCAAAAAG
miR-940	ACACTCCAGCTGGGAAGGCAGGGCCCCCG

Table S2. The clinical stage and histological diagnosis of lung cancer patients.

Patient number	Age	Sex	Clinical stage	Histological diagnosis
1	64	M	IA	Adenocarcinoma
2	53	M	IB	Squamous cell carcinoma
3	43	F	IA	Adenocarcinoma
4	61	F	IB	Adenocarcinoma
5	67	M	IA	Large cell lung carcinoma
6	67	M	IIA	Squamous cell carcinoma
7	74	M	IV	Adenocarcinoma
8	51	M	IIIA	Squamous cell carcinoma
9	79	F	IIIA	Adenocarcinoma
10	66	F	IA	Adenocarcinoma